

Design Fabrication & Real Time Vision Based Control of Gaming Board

Muhammad Nauman Mubarak, Adeel Mehmood, Muhammad Zubair, Zahid Hassan

*Department of Mechatronics Engineering College of EME, National University of Sciences & Technology, Islamabad, 44000, Pakistan
E-mail: mnauman_mts@yahoo.com, adeel_mts@hotmail.com, zubairaw@yahoo.com, zahid_gosh@yahoo.com*

Abstract— This paper presents design, fabrication and real time vision based control of a two degree of freedom (d.o.f) robot capable of playing a carom board game. The system consists of three main components: (a) a high resolution digital camera (b) a main processing and controlling unit (c) a robot with two servo motors and striking mechanism. The camera captures the image of arena and transmits it to central processing unit. CPU processes the image and congregate useful information using adaptive histogram technique. Congregated information about the coordinates of the object is then sent to the RISC architecture based microcontroller by serial interface. Microcontroller implements inverse kinematics algorithms and PID control on motors with feedback from high resolution quadrature encoders to reach at the desired coordinates and angles. The striking unit exerts a controlled force on the striker when it is in-line with the disk and carom hole (or, pocket). The striker strikes with the disk and pots (to hit (a ball) into a pocket) it in the pocket. The objective is to develop an intelligent, cost effective and user friendly system that fulfil the idea of technology for entertainment.

Keywords— Microcontroller; Inverse kinematics; Robotics; Image processing; Simulations.

I. INTRODUCTION

The idea of using technology for entertainment purposes is a hit research area in the fields of Robotics. The concept of using the robots for recreational purposes, besides educational and research purposes, is gaining attention all over the world. Different robotics Competitions are constantly arranged all over the world showing robots performing different interesting tasks for example, ABU Robocon, contest to carry out interesting tasks given to robot [12] Robocup, robot playing football. Such events are providing not only the entertainment but are also very handy for technological evolution [13].

The concept of developing a gaming board is to build some intelligent system capable of playing carom board game. Robot manipulator made for this purpose is a two (d.o.f) degree of freedom PR robot. Two servo motors are used in the design, one motor to produce the translational motion along the x-axis while the other produces rotational motion about z-axis. These motors are DC coreless, rated at 12 V and a no-load speed of 3800 rpm with peak torque 300 mNm. The optical shaft encoder that is mounted on each motors shaft gives the feedback control to the main processing unit i.e. a RISC based microcontroller, the Atmel AtMega16. A Pentium based processor is used for image processing.

A video camera is used to acquire video and the code has been developed on assumption of uniform background using adaptive histogram based edge detection method. A video camera acquire real time video stream and an algorithm searches the video for predefined objects to calculate their location relative to reference axes [9].

Once the position coordinates with respect to reference have been calculated, angles for each respective disk are determined using the algorithm based on the inverse kinematics. DH-parameters based modeling of the robot is used to apply inverse kinematics (See for example [1], [2] and [6]). Study of position control is main concern of the work, so derivation of Jacobian, for velocity control is beyond the scope of this work [4] The decision and priority to pot the disk is based on its proximity to the striker or to the hole, and then near to home position of the robot manipulator.

The scaled down robot is developed as a prototype to implement and prove image processing based control concepts. To achieve precise, accurate and stable system, PID control has been implemented on each motor. A complete system diagram is shown in Fig. 1.

In section 2, mechanical design of the robot is discussed. Position of all the motors and position of capturing device is discussed in detail in this section. In section 3, inverse kinematics algorithm of the PR robot manipulator is

presented. In section 4, electrical hardware required for the robot manipulator is discussed. In section 5, histogram based image processing technique has been elaborated.

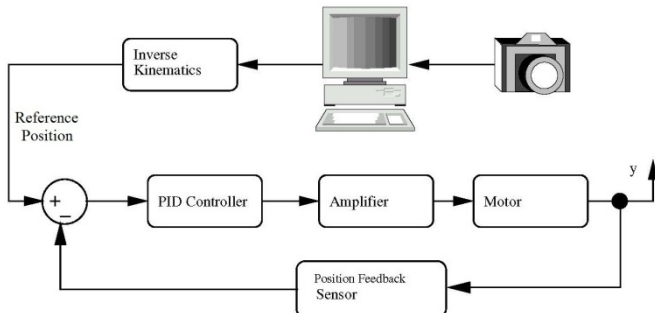


Fig. 1 Complete flow diagram of the system

In section 6, robot simulator is shown to understand model performance and application of control laws on the actual robot.

II. MECHANICAL HARDWARE DESIGN

The manipulator is limited to two linked manipulator with one prismatic and one revolute joint. The material used is Mild steel and Aluminum. Dimensions of the base hardware are (0.61 x 0.18 x 0.12). Fig. 2 shows the fabricated manipulator base and striking unit. Fig. 3 shows the same manipulator designed in the Pro/Engineer environment.

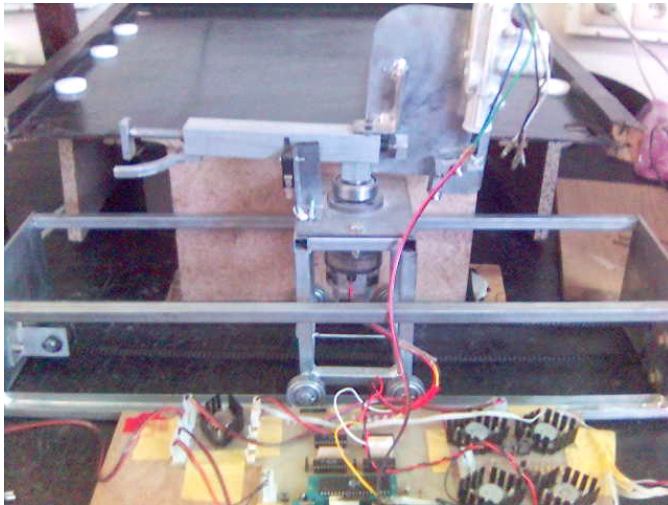


Fig. 2 Robot fabricated manipulator

The mechanical structure is divided into two parts, base hardware and the striking unit. The base hardware holds the striking unit. A motor with incremental encoder mounted on the base unit is connected to the striking mechanism through chain transmission. The use of spur gear with the gearing ratio of 20 teeth to 48 teeth reduces the speed of the motor from 3800 rpm to 1583 rpm at no load. The striking unit consists of the rotational motor, assembly that contains striking plunger and locking motor. A motor to produce the rotation of the striking mechanism is directly coupled with the mechanism because in this way it offers more control and ease to stop the motor at a particular desired angle.

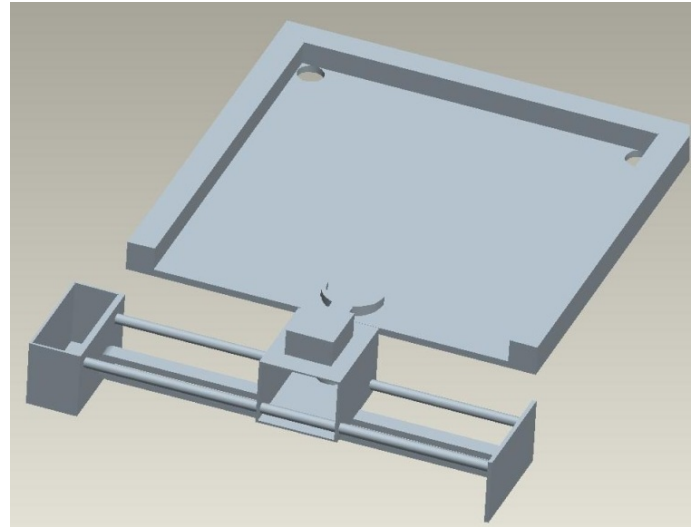


Fig. 3 Pro-Engineering Model of robot manipulator

The rotational motor is restricted to 180 degree with a bumper system. An encoder is also mounted on the rotational motor to acquire position feedback. The locking motor gives both the pushing and pulling force if supplied the alternative voltages. The locking of the striker is done with the help of hooking mechanism that operates when locking motor is given 12 V and on unlocking the clinched parts of hooking mechanism set the striking mechanism plunger free to move in the translational direction due to the preloaded spring force stored in it. This force is transferred to the striker that further strikes the target to pot it in the carom hole. The use of four rods and the railing path for the rotational assembly ensures its smooth motion. The use of ball bearing future lessens the load on the motors.

III. INVERSE KINEMATICS

Inverse kinematics is the motion planning technique to obtain the desired position of end-effector by calculating position of the each link. To apply inverse kinematics on the PR planer manipulator, Robot with one prismatic and one revolute joint, first we need to calculate transformation matrix of this manipulator. Transformation matrix can be calculated with the help of Denavit-Hartenberg (D-H) parameters which describe the placement of the frame of references to find the end-effector position. Fig. 4 illustrates all frame of references connected to the manipulator and there movement. Z-axis is considered as axis of rotation or translation.

Four DH parameters contain all the required information of the manipulator links and joints. DH parameters for this particular PR type manipulator are given in the Table 1. Transformation matrix describes the relationship

TABLE I
PARAMETERS VALUES FOR PNEUMATIC ACTUATORS

i	a_{i-1}	α_{i-1}	d_i	θ_i
1	0	90	d	0
2	0	90	0	θ
3	a	0	0	90

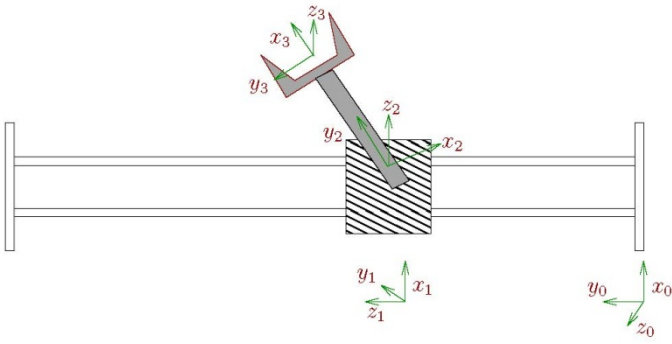


Fig. 4 PR Manipulator with all the frames to calculate DH-parameters

Between the initial and final position of robot manipulator, generalized form of transformation matrix with all DH-parameters is given below

$${}^{i-1}T_i = \begin{bmatrix} \cos \theta_i & \sin \theta_i & 0 & a_{i-1} \\ \sin \theta_i \cdot \cos \alpha_{i-1} & \cos \theta_i \cdot \cos \alpha_{i-1} & -\sin \alpha_{i-1} & -\sin \alpha_{i-1} d_i \\ \sin \theta_i \cdot \sin \alpha_{i-1} & \cos \theta_i \cdot \sin \alpha_{i-1} & \cos \alpha_{i-1} & \cos \alpha_{i-1} d_i \\ 0 & 0 & 0 & 1 \end{bmatrix} \quad (1)$$

Using transformations from global axis to the final axis position for the PR manipulator will lead to the matrix shown in Eq. (2).

$${}^0T_3 = \begin{bmatrix} -\sin \theta & -\cos \theta & 0 & a \cos \theta \\ \cos \theta & -\sin \theta & 0 & a \sin \theta + d \\ 0 & 0 & 1 & 0 \\ 0 & 0 & 0 & 1 \end{bmatrix} \quad (2)$$

Considering that manipulator is at origin with position $P_0(x_0, y_0, z_0)$ and the final position $P_1(x_3, y_3, z_3)$. We can write the manipulator equation with the help of transformation matrix T

$$\begin{bmatrix} x_3 \\ y_3 \\ z_3 \\ 1 \end{bmatrix} = \begin{bmatrix} -\sin \theta & -\cos \theta & 0 & a \cos \theta \\ \cos \theta & -\sin \theta & 0 & a \sin \theta + d \\ 0 & 0 & 1 & 0 \\ 0 & 0 & 0 & 1 \end{bmatrix} \begin{bmatrix} x_0 \\ y_0 \\ z_0 \\ 1 \end{bmatrix} \quad (3)$$

Solving the above matrix equation with known $P_0(x_0, y_0, z_0)$ and $P_1(x_3, y_3, z_3)$, we can calculate variable parameters, translation of the manipulator θ and rotation of the manipulator by the following equations

$$a \cdot \cos \theta - x_0 \cdot \sin \theta - y_0 \cos \theta = x_3 \quad (4)$$

And,

$$d + a \sin \theta - x_0 \cdot \cos \theta - y_0 \sin \theta = y_3 \quad (5)$$

IV. ELECTRICAL HARDWARE DESIGN

Low cost printed circuit boards are designed and manufactured using OrCAD 9.2. Electrical hardware comprises micro-controller AtMega16, two motor drives (H-Bridge) and one Electronic switch used to energize the motor for striking mechanism. Different electrical subsystems are described below.

A. Micro-controller

Atmel AtMega16 is a high performance, low power, 8 bit micro-controller having an on chip programmable flash memory of 16 KB and 1024 bytes of SRAM, 4 PWM channels all of which are used to control two motors and 3 external interrupts which are used for reading the encoders. The controller has two modes of serial communication, the standard USART and the SPI protocol for master slave configuration. AtMega16 has a maximum throughput of 16 MIPS. Based on the RISC architecture, most of the commands are executed on single clock cycles (See for example [11]). The combination of these features makes the controller suitable for control applications.

B. Motors and Their Drives

The motors used are Buhler motors that supply 24 Vdc and have six wires, two of which are used for motor power other four wires are used for optical encoder (GND, VCC, Phase A, Phase B). Two motors, one for prismatic joint and other for revolute joint link, are derived with H-bridges. Each H-bridge consists of four Darlington pairs. Each Darlington pair, made by a PNP transistor 3904 and a MOSFET 2N3055, can amplify the current up to 10 Amp. Input is PWM signal that controls the speed of the motor. A separate switch is used to energize the motor used in the striking mechanism. Complete electronic circuitry is shown in Fig. 5.

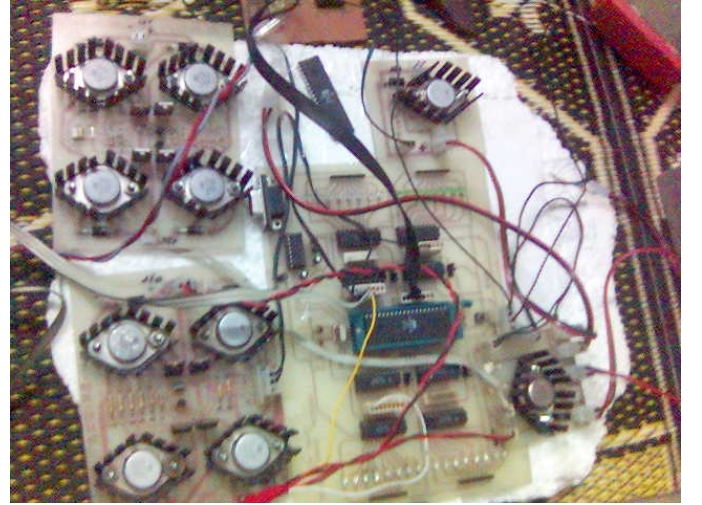


Fig. 5 Complete electronic circuitry of the PR robot manipulator

C. Quadrature Encoders

Each of the motors used has built in quadrature encoders. The optical encoder is two phase encoder with the capability to determine the direction of the motor by comparing the phase of the square waves. The encoders generate square waves at a frequency proportional to the angular velocity of the motor shaft. There is a phase difference of 90 between the waveforms of each of the two encoders. Optical encoder mounted on Buhler motor is shown in Fig. 6. Angle and the displacement calculated by the inverse kinematics algorithm are translated into the encoder counts using the following equation.

$$\delta_{tc} = \frac{\theta_d}{2\pi} (\delta_{rev-c} * g_r) \quad (6)$$

Where δ_{tc} , θ_d , δ_{rev-c} and g_r are total number of encoder counts, desired angle in radian, number of encoder counts per revolution and gear ratio respectively.

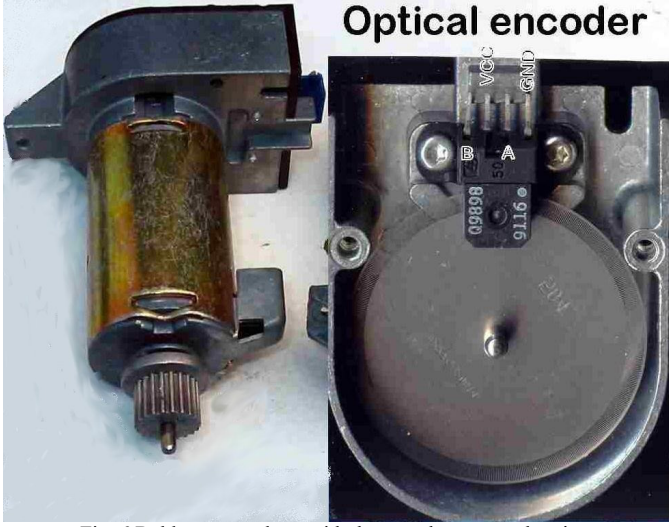


Fig. 6 Buhler motor along with the encoder mounted on it

D. PID Controller

The number of counts thus calculated is treated to determine the error. At time $t=0$ the error is maximum and is equal to the calculated counts. Applied voltage is proportional to the error of position. Greater the error, the greater is the applied voltage. To eliminate steady state error and to avoid unnecessary fluctuation a PID controller is implemented. Ziegler-Nichols tuning method is used to tune the parameters of the PID controller. Error between the actual and desired value is given by

$$e_r(t) = (\delta_d - \delta_{tc}) \quad (7)$$

Where δ_d is the desired angle or position. PID controller in continuous domain is given by

$$u(t) = K_p * e_r(t) + K_i * \int e_r(t) + K_d \frac{de_r(t)}{dt} \quad (8)$$

Where K_p , K_i and K_d are the proportional, integral and derivative gain of the PID controller. To write discrete time equation, we need to approximate the integral and the derivative terms in the equation (8) to suitable forms for simplicity in computation (7).

$$U_i = K_p * e_r(i) + \frac{K_c T_s}{T_i} \sum e_r(i) + K_c T_d \frac{(e_r(i) - e_r(i-1))}{T_s} \quad (9)$$

V. IMAGE PROCESSING

Algorithm is developed with the assumption of uniform background using adaptive histogram based edge detection method. The pixel data can be constrained based on their relative distance [9], [10]. To detect the circular disks (and holes) in the image by means of an image recognition system, an algorithm capable of recognizing ellipses and computing the coordinates of their centre is required. A pixel is parameterized by position (column, row), intensity (in red, in green, in blue) and time (number of frames).The

values at any point (x,y) is proportional to the intensity (brightness) at that point, where x and y denotes spatial coordinates.

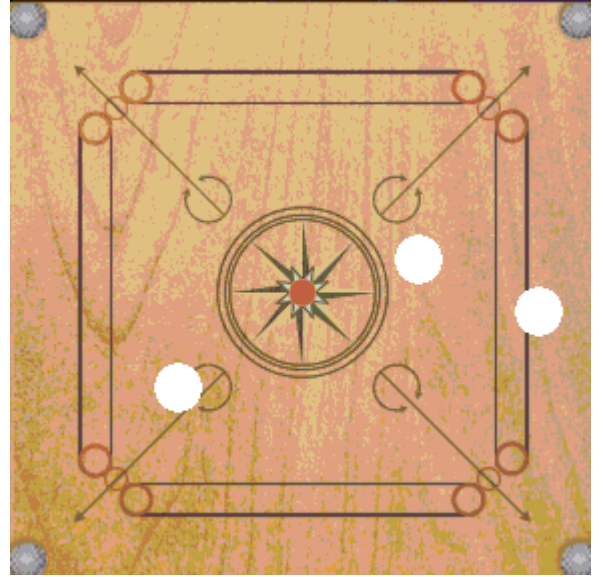


Fig. 7 Image seen by camera for histogram processing technique

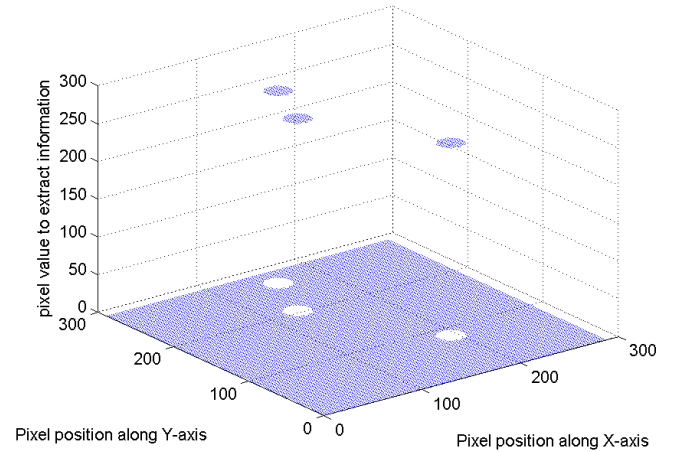


Fig. 8 Computation of position by using histogram processing technique

To implement this, a histogram of pixels forming an ellipse is found with respect to an origin. The coordinates of the centre of the disks is computed. Once, the coordinates of the centre of the disks are computed, a triangle is formed. With the same slope we draw another triangle and calculate the angle of target. The height of the camera lens is measured and not changed during the process. The corresponding pixel is calculated by adjusting camera to a point exactly parallel to the reference point height.

The algorithm assigns either zero to black or 255 to white pixels. Above a threshold value, a pixel is assigned 255 (white pixels) and below a zero value (black pixel) is assigned. In this way we get disks separated from the background of carom board. Threshold is defined as function of minima and maxima and mean value of histogram that allows the algorithm to cope with environmental effects. Fig. 9 shows the short selection criteria for more than one object. Short selection for more than one object is done on the preference of minimum

distance between hole and disk or minimum distance required to hit the target. Once the coordinates of the disks are calculated it is sent to the micro-controller by serial port which directs the motors to rotate till the base hardware (having striking mechanism) reaches to the point that is exactly in-line to the centre of the disk and carom board hole. After reaching the position locking motor is given signal that releases the striker which hit the disk(s) and tries to pot it into the hole.

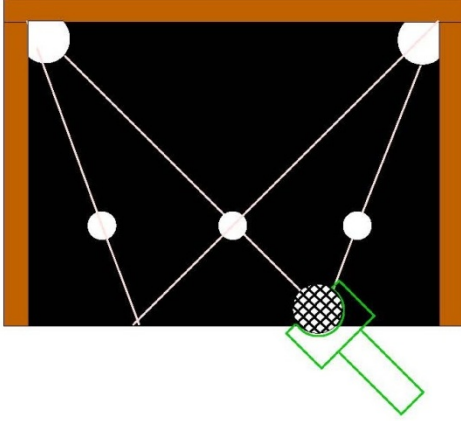


Fig. 9 Short selection criteria defined for the object position on the area

VI. MODELLING AND SIMULATIONS

To perform the simulation of the system, a model based on the motor specifications is established. Relationship between motor current i and torque T_m is given by following equation

$$T_m = k_a i \quad (10)$$

Here k_a is torque constant. Back EMF E_a , generated in the motor is proportional to the angular speed ω of motor. Equation for back EMF is given by

$$E_a = k_m \omega \quad (11)$$

k_m is mechanical constant and it is equal to torque constant if gear ratio is one. Equation of all the torque acting on the motor is given by the following equation

$$I_a \frac{d\omega}{dt} = T_m + T_f \quad (12)$$

Where I_a is the moment of inertia of the motor. T_f is the torque due to coulomb and damping friction. Equation of current passing through armature of the motor is obtained by using the Kirchhoff's voltage law,

$$i = \frac{U_{PWM}}{R} - \frac{E_a}{R} \quad (13)$$

Where U_{PWM} and R are applied PWM voltage and coil resistance, respectively. Combining all equations together and by putting their values in equation (12), we get following equation

$$I_a \ddot{\theta} = k_a \frac{U_{PWM}}{R} - k_a^2 \frac{\dot{\theta}}{R} + T_f \quad (14)$$

A simulator is designed in the Matlab/ Simulink to understand the decision making capabilities of the robot and response of the applied PID controller. Input to the simulator is the coordinate position of the disk. Using this information simulator aligns itself to the target. PID controller is tuned using Ziegler-Nichols method. A simulator for PR robot manipulator is shown in Fig. 12.

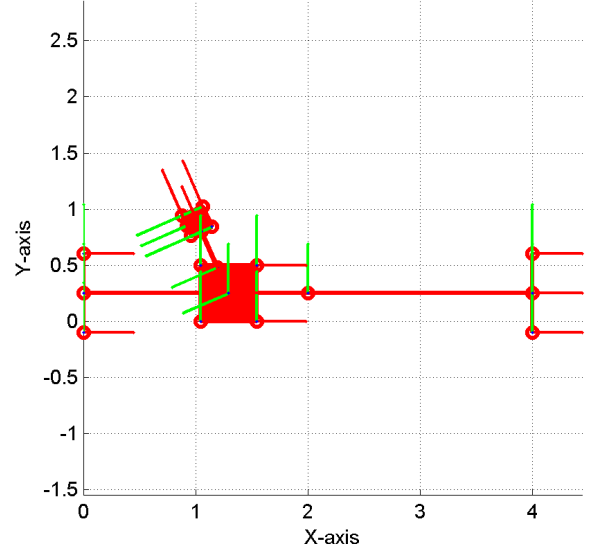


Fig. 10 Simulation for PR robot manipulator has aligned itself to the target direction

Simulator model can be visualized using machine environment block. The Machine Environment block allows us to view and change the mechanical environment settings for our manipulator. A virtual model aligned to the target position is shown in Fig. 10.

Response of the PID controller is compared with the simulation results in Fig. 11. First figure shows the desired and actual position of the link with prismatic joint whereas in second figure reference angle is shown with respect to actual rotational angle of the link connected with revolute joint.

VII. DISCUSSION

The System designed is a prototype aiming the striker to hit one disk at a time. The task has been further made easy by employing the uniform black background utilizing the widely used method of image segmentation i.e. adaptive histogram based edge detection method.

Histogram based methods are considered very efficient when compared to other image segmentation methods because they typically require only one pass through the pixels. Also, they permit us to eliminate external disturbances and are adaptive to the environment. The adaptive histogram based edge detection method best suits our arena and yields efficient results. The efficiency of the chosen method was noted by observing the rate of hitting to disks present in the arena which is quite high (79.4 %, 27 successful hits out of 34 total attempts).

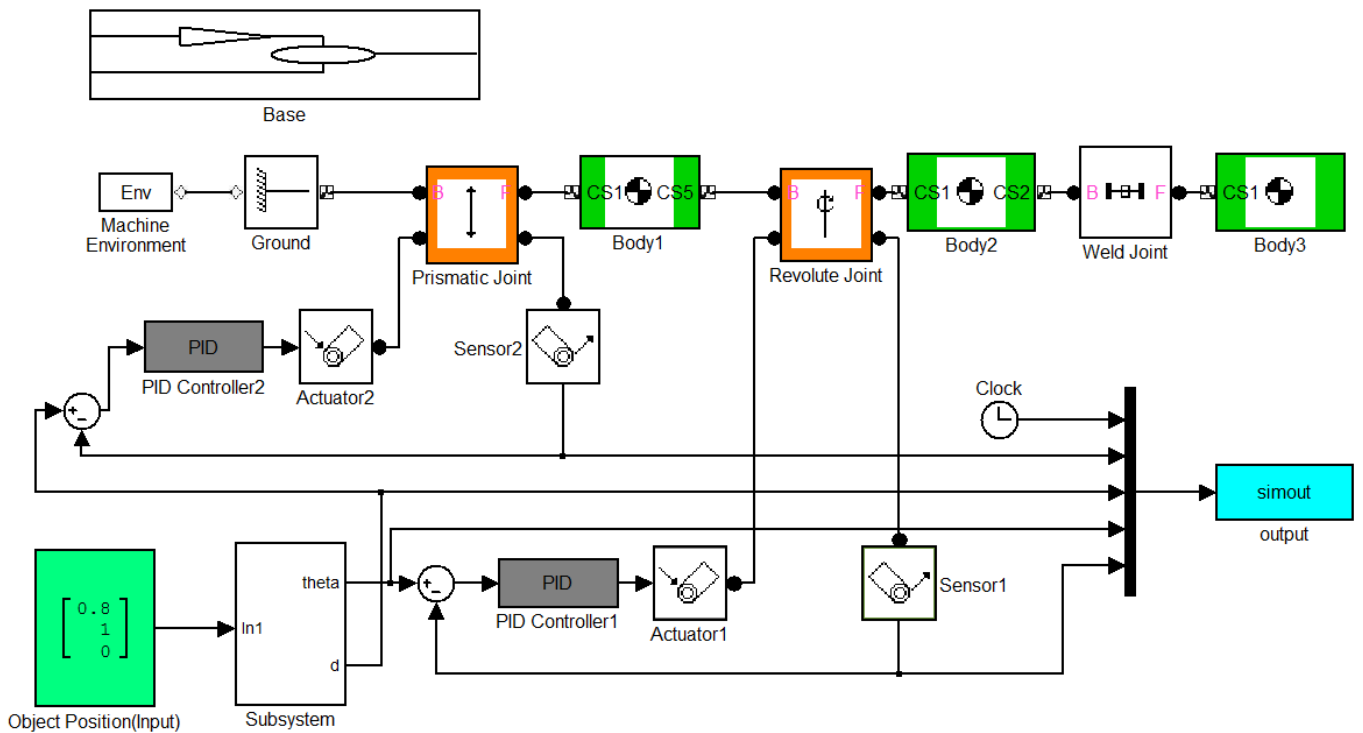


Fig. 12 Simulator for 2 DOF robot manipulator

VIII. CONCLUSIONS

The design and control of an application based project, the garming board robot, is achieved with the help of two motors with position feedback. A separate motor is used to produce striking force. Image is processed by applying adaptive histogram analysis technique that makes the system robust and adaptive to the environment.

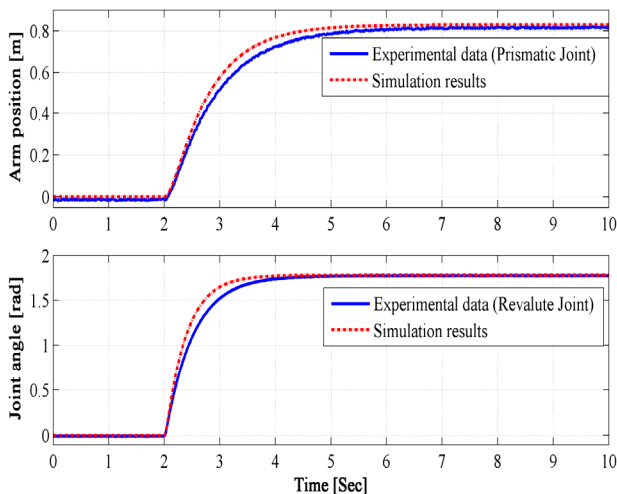


Fig. 11 Simulation and experimental results for PR robot manipulator. First figure shows the prismatic joint and second revolute joint

Robot is intelligent enough to make decisions by itself. Position control has been implemented on the manipulator using high performance RISC architecture based AVR microcontrollers. Control algorithm of the robot can be further improved by putting into practice artificial intelligence and decision making capabilities.

REFERENCES

- [1] J. J. Craig, *Introduction to Robotics, Mechanics and Control*, 2nd Edition published by Wesley, ISBN-13: 9780201095289, 1999.
- [2] C. Crane, J. Duffy *Kinematic Analysis of Robot Manipulators*, 1st Edition published by Cambridge University Press, ISBN-13: 9780521047937, 1998.
- [3] R. Lafore, *Turbo C Programming for the PC*, Revised edition published by prentice hall, ISBN-13:9780672226601, 1988.
- [4] H. Roh, J. Kim, "Manipulator modelling from DH Parameters," *In proc. of 30th Annual Conference of the IEEE Industrial Electronics Society, Busan Korea 2004*.
- [5] M. U. khan, N. Iqbal, "Control of robot arm PA-10 using camera vision," *In Proc. of International Bhurban Conference on Applied Sciences & Technology, pages 97-103, Bhurban Pakistan 2007*.
- [6] E. M. Schwartz, R. Manseur, "Non-commensurate manipulator jacobian," *In Proc. of the IASTED International Conference, Salzburg, Austria 2003*.
- [7] K. Altaf, A. Akhtar, S. Rahman and J. Iqbal, "Design, implementation and real-time digital control of a cart-mounted inverted pendulum using Atmel AVR Microcontroller," *In Proc. of the 6th WSEAS International Conf. on Signal Processing, Robotics and Automation, Greece 2007*.
- [8] S. Kucuk and Z. Bingul, "The Inverse Kinematics Solutions of Industrial Robot Manipulators," *In Proc. Of the IEEE International Conference on Mechatronics, pages 274-279, Turkey 2004*.
- [9] K. Kim, "Algorithms and evaluation for object detection and tracking in computer vision," Phd thesis, University of Mariland, USA, 2005.
- [10] S. Ekvall, D. Kragic, "Receptive Field Co-occurrence Histograms for Object Detection," *In proc. IEEE/RSJ International Conference on Intelligent Robots and Systems, pages 84-89, 2005*.
- [11] "AT Mega16 data sheet," AVR microcontroller 2009, California, USA.
- [12] ABU Robocon 2009, [Online]. Available: <http://www.aburobocon2009.com>
- [13] RoboCup 2009, [Online]. Available: <http://www.robocup2009.org>